Electronic Supplementary Information (ESI)

Nonaqueous electrolyte with dual-cations for high-voltage and long-life zinc batteries

Yang Dong,[a] Shengli Di,[a] Fangbo Zhang,[a] Xu Bian,[a] Yuanyuan Wang,[a] Jianzhong Xu,*[a] Liubin Wang,[b] Fangyi Cheng[b], and Ning Zhang*[ab]

[a] *College of Chemistry & Environmental Science, Key Laboratory of Analytical Science and Technology of Hebei Province, Hebei University, Baoding 071002, China. E-mail: xujz@hbu.edu.cn; ningzhang@hbu.edu.cn*

[b] *Key Laboratory of Advanced Energy Materials Chemistry (Ministry of Education), Renewable Energy Conversion and Storage Center, College of Chemistry, Nankai University, Tianjin 300071, China.*

Experimental Section

Materials. NVPOF was synthesized by a solvothermal method. Typically, NH_4VO_3 (0.242 g), $NH_4H_2PO_4$ (0.230 g), $Na_2CO_3 \cdot H_2O$ (0.124 g), and NaF (0.042 g) with a molar ratio of 2:2:1:1 were dissolved into 12 mL distilled water. The mixture was added into 30 mL N,N-dimethylformamide (DMF) solvent and its pH was adjusted to 7 with HNO_3. The mixed solution was loaded into a 50 mL Teflon-lined autoclave and maintained at 150 ^oC for 20 h. The obtained NVPOF powders were centrifuged, washed thoroughly using water and ethanol, and dried at 100 ^oC for 10 h. Metallic Zn foil, $Zn(OTf)_2$, $NaClO_4$, and TMP were purchased from *Aladdin.* Electrolytes were prepared by dissolving the desired amount of salts in the selected solvents in a glove-box.

$Na_3V_2(PO_4)_2F_3$ was synthesized by a solvothermal method. Typically, 359.0 mg $V(C_5H_7O_2)_3$ was dissolved in 3 mL ethanol and 1 mL acetone. And then 104 uL H_3PO_4 (85%) was added to this solution, followed by addition of 71.5 mg NaF powder. The obtained mixture was ultrasound-treated for 10 min, then transferred into a Teflon cup with inner volume of 30 mL, placed in a steel autoclave, and carefully sealed. The autoclave was heated in a furnace at 180 ^oC for 20 h. The obtained $Na_3V_2(PO_4)_2F_3$ powders were centrifuged, washed thoroughly using water and ethanol, and dried at 80 ^oC for 10 h.

In a typical synthesis of $Na_3V_2(PO_4)_3$, 4 mmol V_2O_5, 12 mmol $NH_4H_2PO_4$ and 6 mmol Na_2CO_3 were added to 70 mL of distilled water and magnetically stirred at room temperature. Then, 6 mmol ascorbic acid and 6 mL of polyethylene glycol 400 were added to form a blue suspension, which was stirred for 60 min before being transferred to a 100 mL Teflon-lined auto-clave. The sealed autoclave was kept at 180 ^oC for 20 h. The resulting brown mixture was ultrasonically treated for 90 min to make a uniform dispersion, and then heated on a hot plate at 95 ^oC with stirring to evaporate water. The obtained brown sol was dried at 120 ^oC overnight. This precursor was thoroughly ground and pre-heated at 350 ^oC for 4 h. The preheated sample was ground to powders and finally calcined at 750 ^oC for 6 h in flowing Ar atmosphere.

Characterization. XRD patterns were performed on a Bruker D8 ADVANCE (Cu Kα radiation). SEM images were obtained on a Field-emission JEOL JSM-7500F microscope. TEM images and EDS profiles were taken on a Talos F200x G2 microscope, AEMC. XPS, Raman, and FTIR spectra were performed on a PHI 1600 ESCA spectrometer (Perkin-Elmer), a confocal Thermo-Fisher Scientific DXR microscope using 532 nm excitation, and a Nicolet iS10 spectrometer (Thermo-Fisher Scientific), respectively. The viscosity of electrolyte was measured by an MDJ-5S viscometer (Shanghai, China) at 25 °C. The UV-vis absorption spectra were recorded by a Shimadzu UV-3600 spectrometer at room temperature. Thermogravimetric (TG) analyses were conducted on a Netzsch STA 449C thermal analyzer under N_2 atmosphere from 35 to 350 ^oC with a heating rate of 10 ^oC min^{-1}. ICP-AES measurements were conducted on a PerkinElmer Optima 8300.

Electrochemical tests. The Zn plating/stripping behaviours in TMP-based electrolytes were characterized by cyclic voltammograms (CVs) at a rate of 0.5 mV s^{-1} using Ti foil as the working electrode and Zn foils as the reference and counter electrodes. The CE values of Zn stripping/plating were measured using Zn/Ti cells with a cut-off charging potential of 0.8 V. Symmetric Zn/Zn cells were employed to evaluate the reversibility and stability of the TMP-based electrolytes. Electrochemical performances of the Zn/NVPOF batteries in TMP-based electrolytes were tested using CR2032 coin-type cells with NVPOF cathode, glass fiber separator, and Zn foil anode. The working electrode was fabricated by blending NVPOF powder, Super P carbon, and sodium carboxymethyl cellulose (CMC) binder in a weight ratio of 8:1:1 using water as solvent. The obtained slurry was pasted onto Ti foil or stainless steel foil, and vacuum-dried at 80 ^{o}C for 10 h. The as-prepared electrode was cut into round slices and the typical mass loading of active materials was ~2 mg cm^{-2}. The zinc anode was prepared by mixing 80% zinc powder, 10% Super P carbon, and 10% CMC using water as solvent and the slurry mixture was then coated on stainless steel foil. Charge/discharge testing was measured on a LAND-CT2001A battery-testing instrument. The specific capacities were based on the active mass. EIS and CVs were performed on a CHI660E electrochemical work station and the frequency in EIS test was set from 100 kHz to 50 mHz with an ac perturbation signal of 5 mV.

Supporting Figures

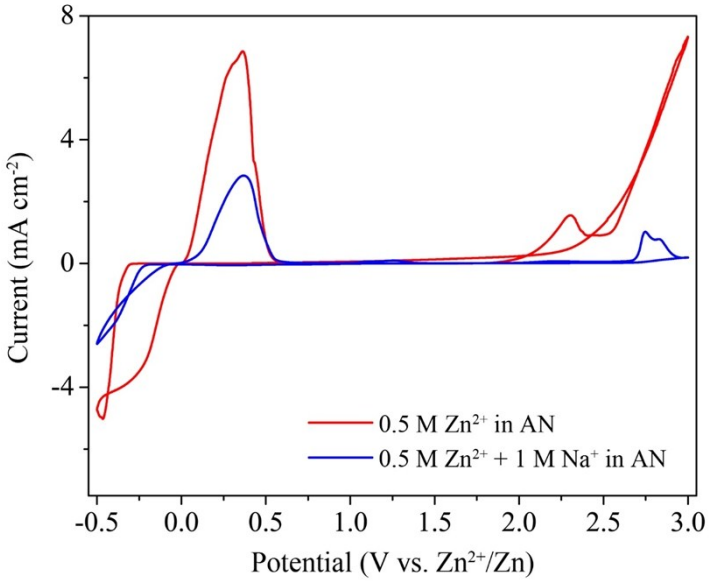

Fig. S1 CV profiles of Zn/Ti cells using AN-based electrolytes (e.g., 0.5 M Zn^{2+} in AN and 0.5 M Zn^{2+} + 1.0 M Na^{+} in AN) at 0.5 mV s^{-1}.

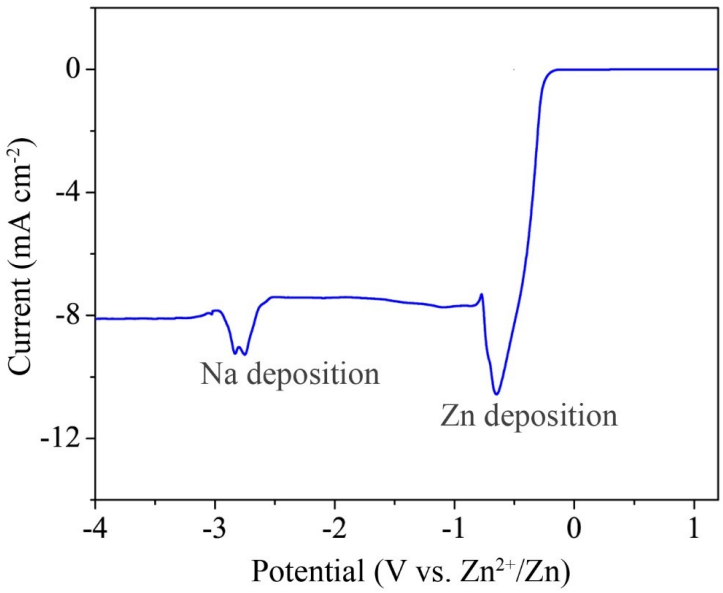

Fig. S2 Linear sweep voltammetry (LSV) profile of the 0.5 M Zn^{2+} + 1.0 M Na^{+} electrolyte in a three-electrode cell using Ti foil as a working electrode and Zn foils as the reference and counter electrodes at 0.5 mV s^{-1} from 1.2 to -4.0 V (vs. Zn^{2+}/Zn). The onset potentials of Zn deposition and Na deposition are -0.27 V (vs. Zn^{2+}/Zn) and -2.50 V (vs. Zn^{2+}/Zn; i.e., -0.55 V vs. Na^{+}/Na), respectively.

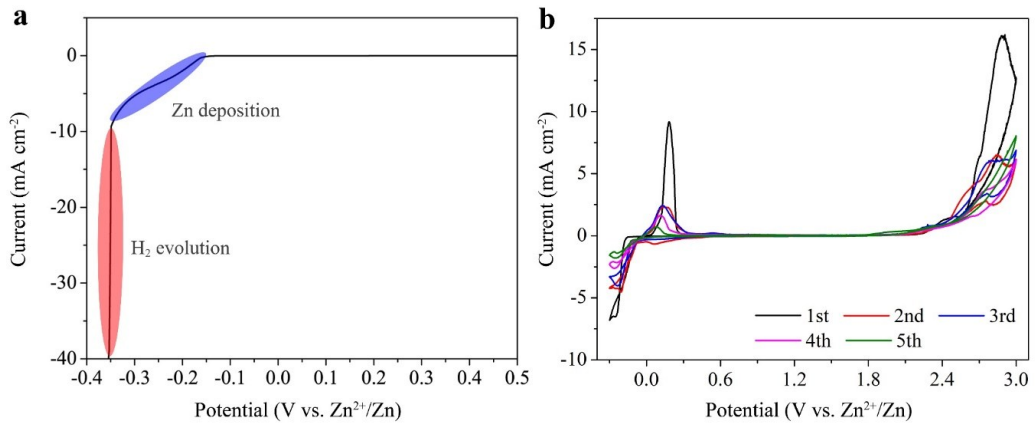

Fig. S3 Electrochemical stability of the aqueous 0.5 M Zn^{2+} + 1.0 M Na^{+} electrolyte. (**a**) Linear sweep voltammetry (LSV) profile of the 0.5 M Zn^{2+} + 1.0 M Na^{+} aqueous electrolyte in a three-electrode cell using Ti foil as a working electrode and Zn foils as the reference and counter electrodes at 0.5 mV s^{-1} from 0.5 to -0.355 V. (**b**) CV curves of the Zn/Ti cell at 0.5 mV s^{-1} within the voltage window between -0.3 and 3.0 V. The aqueous electrolyte shows a seriously hydrogen evolution under -0.34 V and an oxygen evolution reaction up to 2.3 V (vs. Zn).

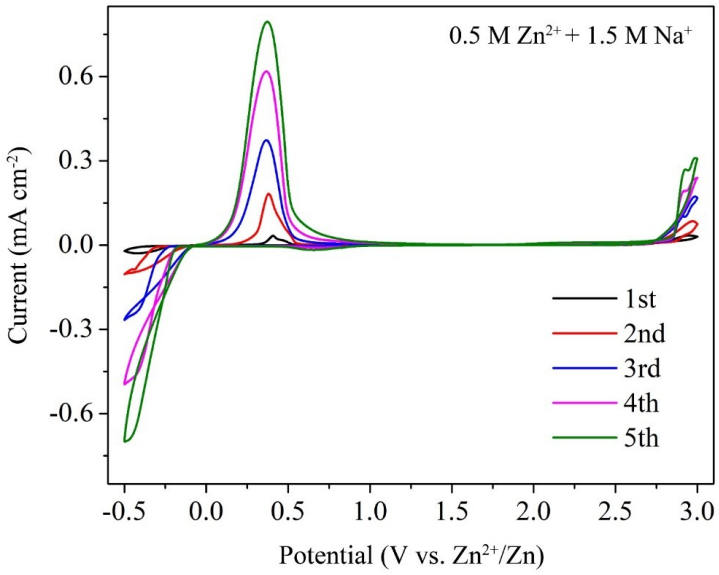

Fig. S4 CV profiles of the Zn/Ti cell using the 0.5 M Zn^{2+} + 1.5 M Na^{+} electrolyte at a scan rate of 0.5 mV s^{-1} within the voltage window of -0.5–3.0 V.

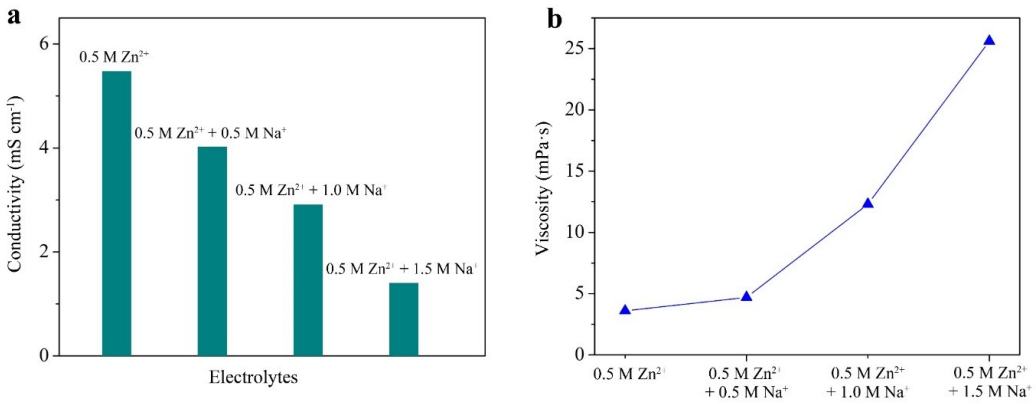

Fig. S5 (**a**) Ionic conductivities and (**b**) viscosities of 0.5 M Zn^{2+}, 0.5 M Zn^{2+} + 0.5 M Na^{+}, 0.5 M Zn^{2+} + 1.0 M Na^{+}, and 0.5 M Zn^{2+} + 1.5 M Na^{+} electrolytes.

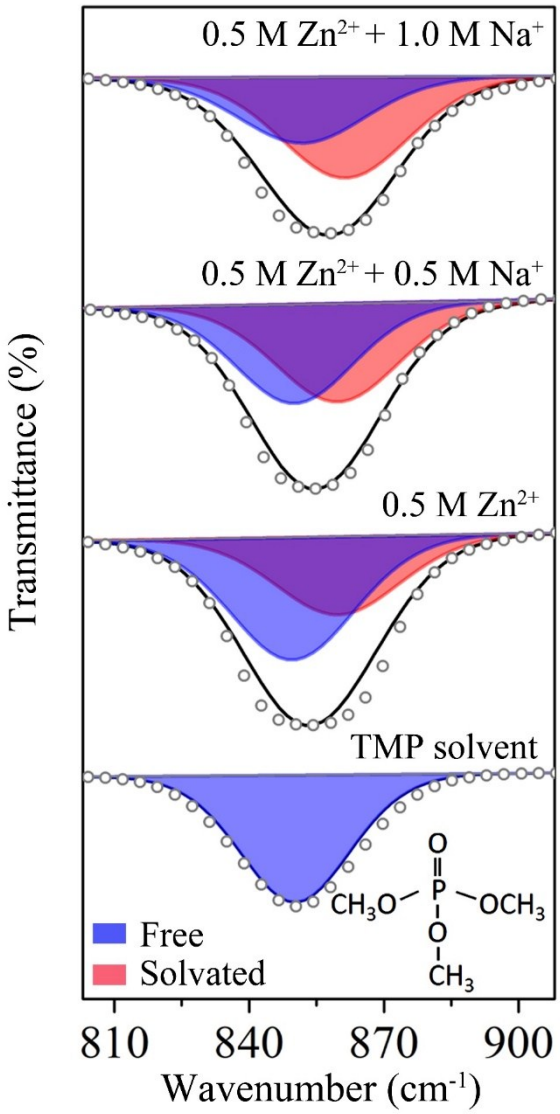

Fig. S6 FTIR spectra between 803 and 908 cm^{-1} (P-O-(C) stretching mode) of the pure TMP solvent, and the 0.5 M Zn^{2+} TMP-based electrolytes with different Na^{+} concentrations.

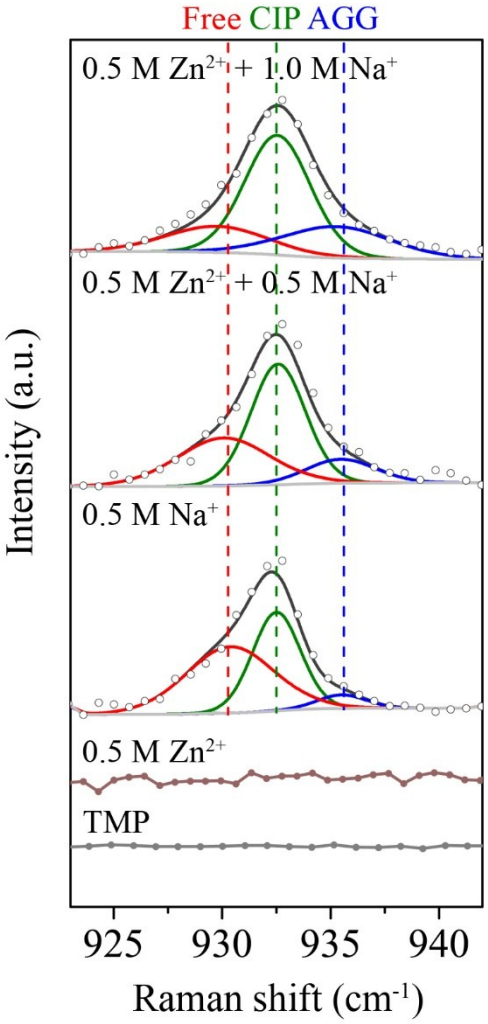

Fig. S7 Raman spectra between 925 and 940 cm^{-1} (vibration mode of ClO_4^- anions) of the pure TMP solvent, and the 0.5 M Zn^{2+} TMP-based electrolytes with different Na^+ concentrations.

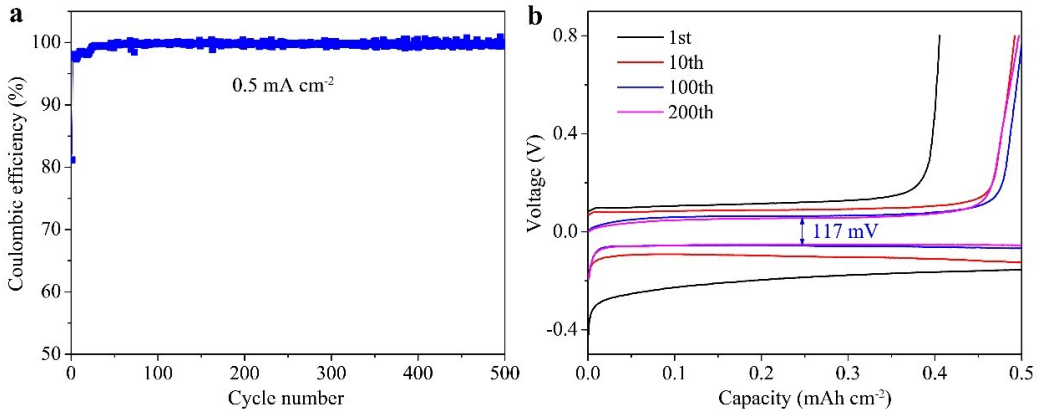

Fig. S8 Zn plating/stripping performance of Zn/Ti cell in 0.5 M Zn^{2+} + 1.0 M Na^{+} electrolyte at 0.5 mA cm^{-2} with a plating time of 1 h. (**a**) Coulombic efficiencies and (**b**) selected voltage profiles.

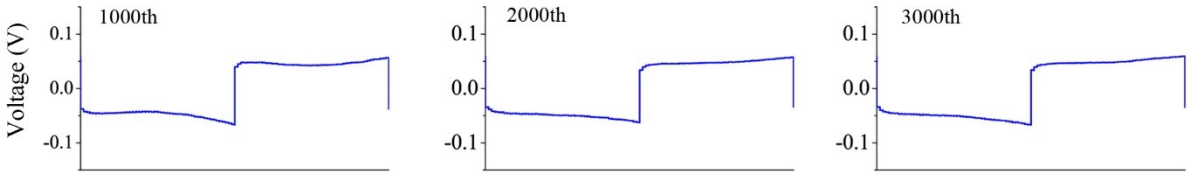

Fig. S9 Zn plating/stripping profiles. Zn plating/stripping curves at the 1000th, 2000th, and 3000th cycles at 0.5 mA cm^{-2}.

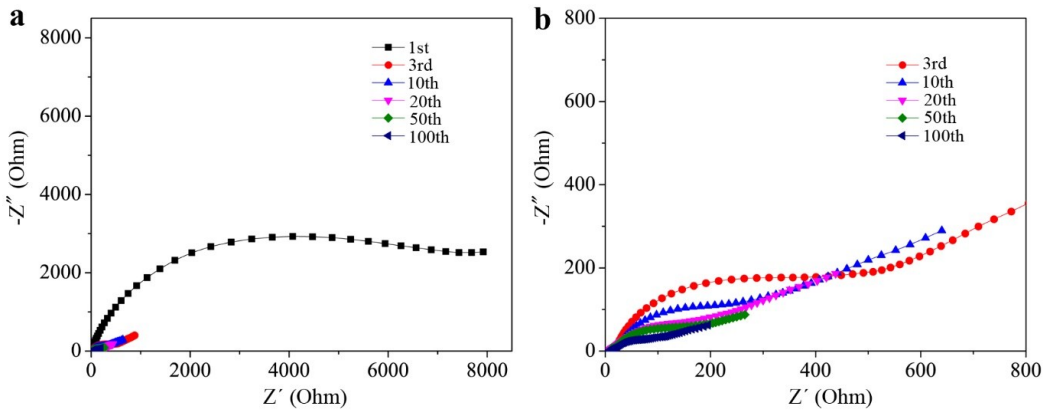

Fig. S10 (**a**) EIS spectra and (**b**) the enlarged profiles of the Zn/Zn cell during the Zn plating/stripping test.

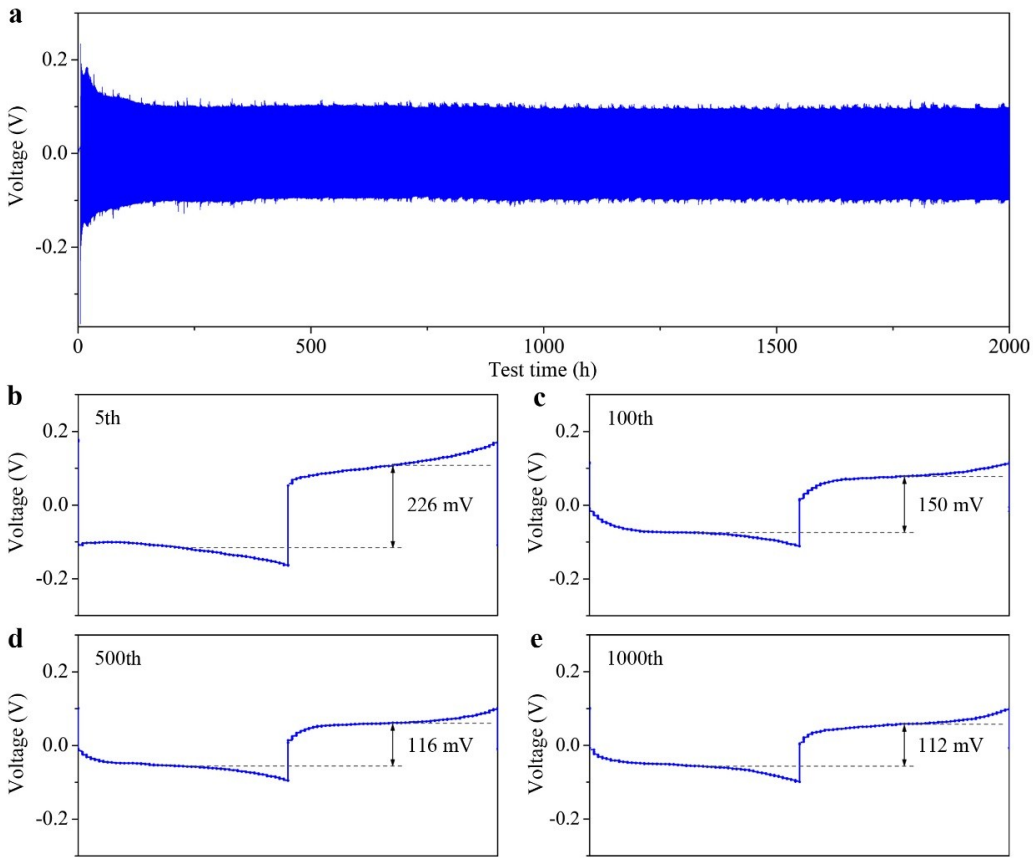

Fig. S11 Cycling performance of Zn/Zn symmetrical cell in 0.5 M Zn^{2+} + 1.0 M Na^{+} electrolyte at 1.0 mA cm^{-2}. (**a**) Galvanostatic Zn plating/stripping profiles. (**b-e**) Enlarged Zn plating/stripping curves at the 5th, 100th, 500th, and 1000th, respectively.

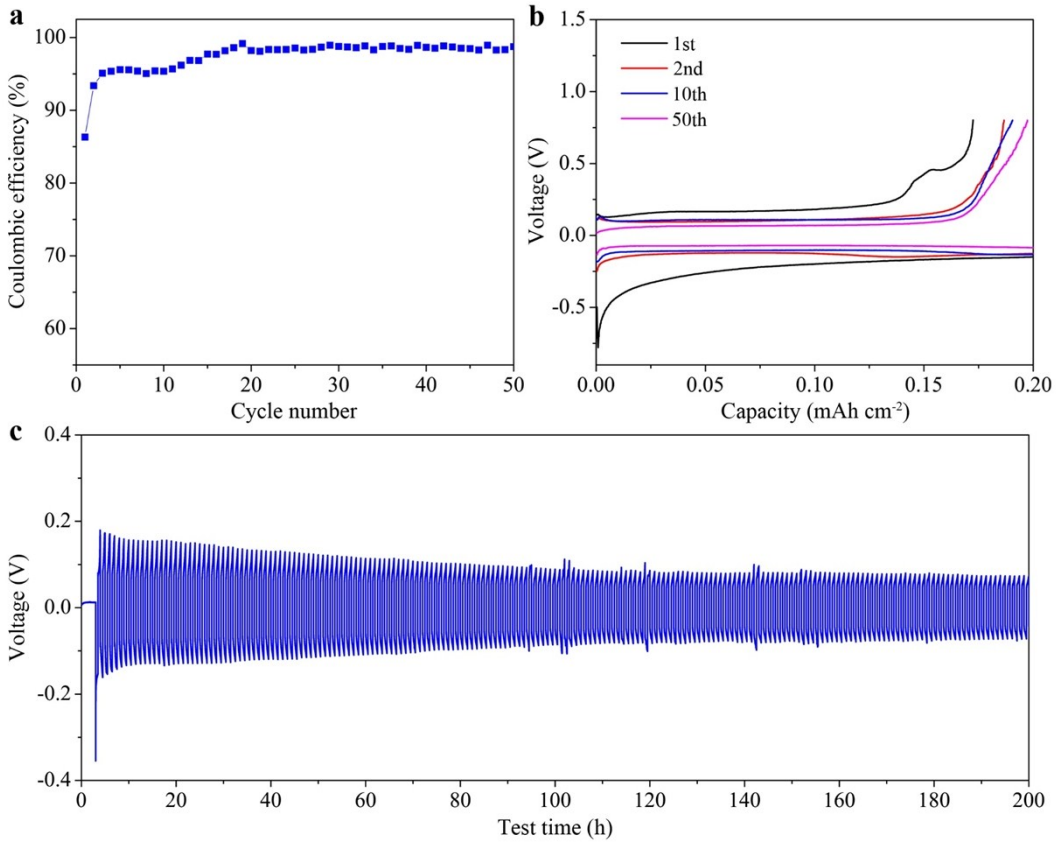

Fig. S12 (**a**) Coulombic efficiencies and (**b**) voltage profiles of the Zn-Ti cell using 0.5 M Zn^{2+} + 1.0 M Na^{+} in AN electrolyte at 0.2 mA cm^{-2} with a deposition time of 1 h. (**c**) Cycling performance of Zn/Zn symmetrical cell using 0.5 M Zn^{2+} + 1.0 M Na^{+} in AN electrolyte at 0.5 mA cm^{-2} with a discharge/charge time of 0.5 h.

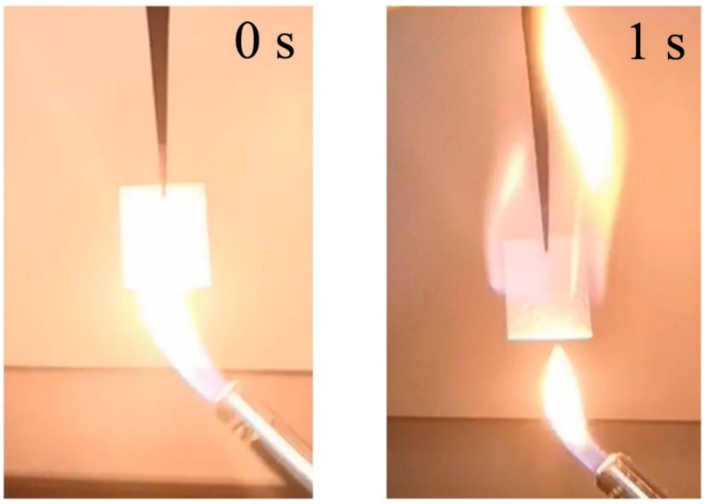

Fig. S13 Photographs of the ignition test of a glass fiber saturated with the 0.5 M Zn^{2+} + 1.0 M Na^{+} in AN electrolyte.

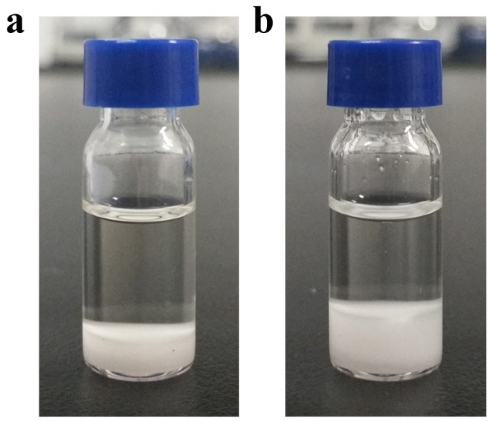

Fig. S14 Digital photos of the carbonate-based electrolytes. (**a**) 0.5 M Zn^{2+} + 1.0 M Na^{+} in propylene carbonate **(**PC**)** and (**b**) 0.5 M Zn^{2+} + 1.0 M Na^{+} in ethylene carbonate/diethyl carbonate (EC/DEC, volume ratio: 1:1). Clearly, the salts cannot fully dissolve into the PC or EC/DEC solvents.

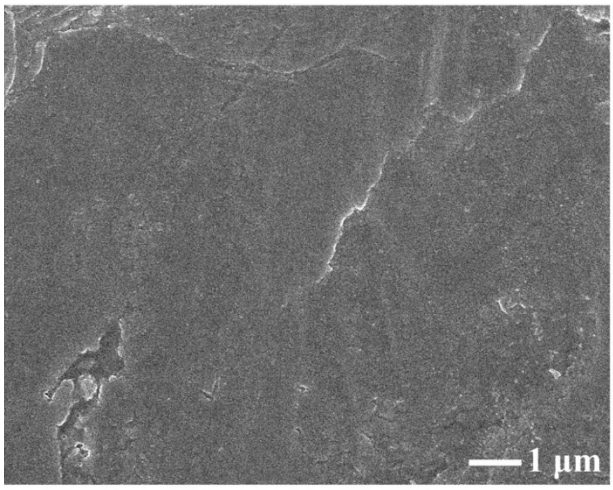

Fig. S15 SEM images of the pristine Zn anode.

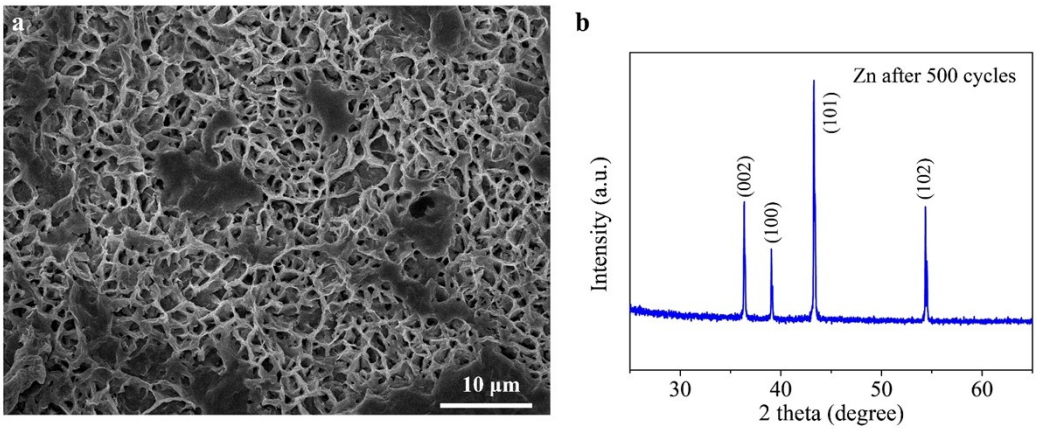

Fig. S16 Zn anode characterization. (**a**) Low-magnification SEM image and (**b**) XRD pattern of the Zn anode after 500 cycles.

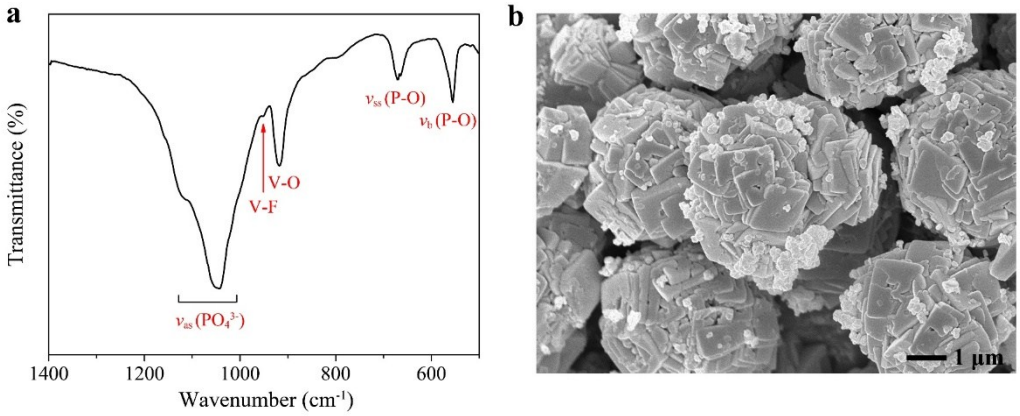

Fig. S17 Characterizations of the as-prepared NVPOF. (**a**) FTIR spectrum and (**b**) SEM image.

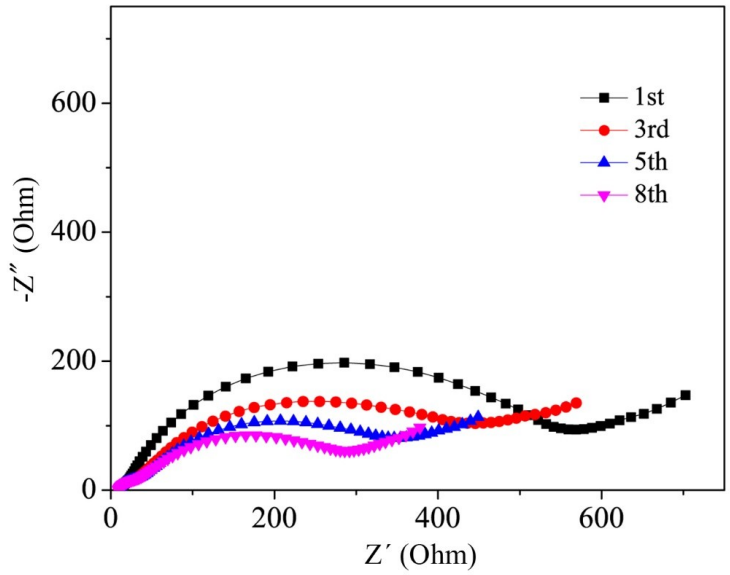

Fig. S18 EIS spectra of the Zn/NVPOF cell during cycling.

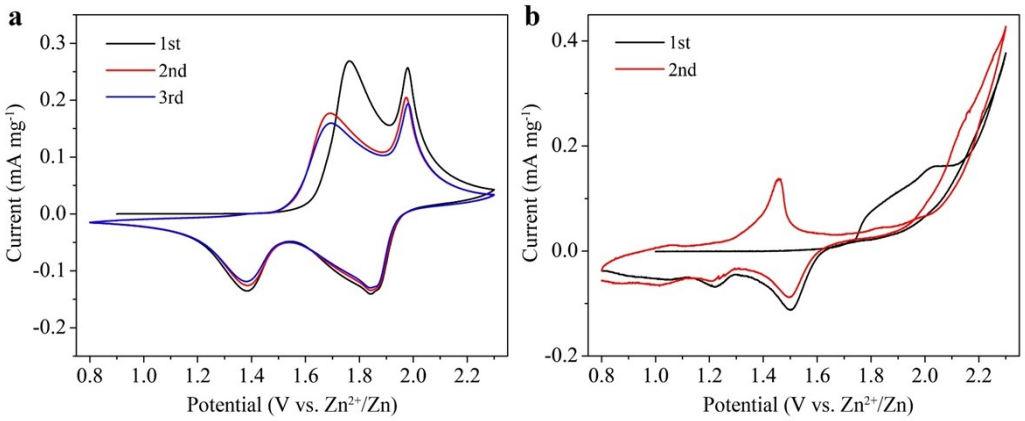

Fig. S19 CV curves of NVPOF cathode in (**a**) AN-based electrolyte (i.e., 0.5 M Zn^{2+} + 1.0 M Na^{+} in AN) and (**b**) aqueous electrolyte (i.e., 0.5 M Zn^{2+} + 1.0 M Na^{+} in water) at 0.2 mV s^{-1}.

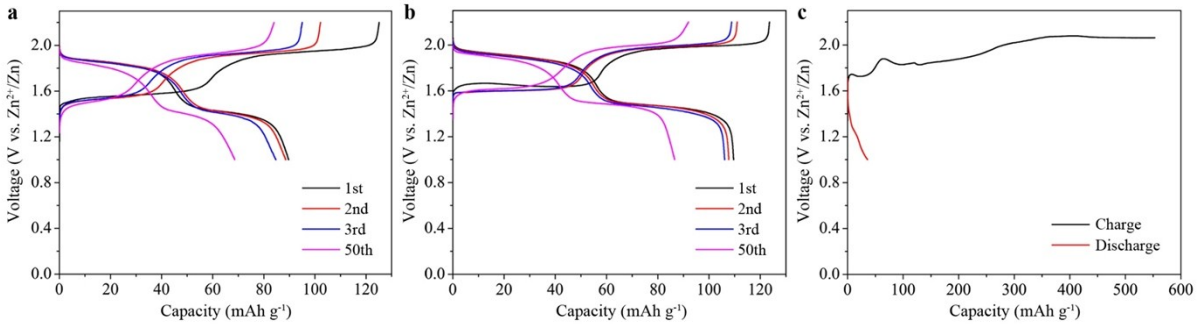

Fig. S20 Selected charge/discharge curves of the Zn/NVPOF cell in (**a**) 0.5 M Zn^{2+} TMP-based electrolyte at 0.2 C, (**b**) 0.5 M Zn^{2+} + 0.5 M Na^{+} TMP-based electrolyte at 0.2 C, and (**c**) aqueous 0.5 M Zn^{2+} + 1.0 M Na^{+} electrolyte at 0.5 C. The cell cannot work in the aqueous 0.5 M Zn^{2+} + 1.0 M Na^{+} electrolyte between 1.0 V and 2.2 V, due to the poor stability of aqueous electrolyte.

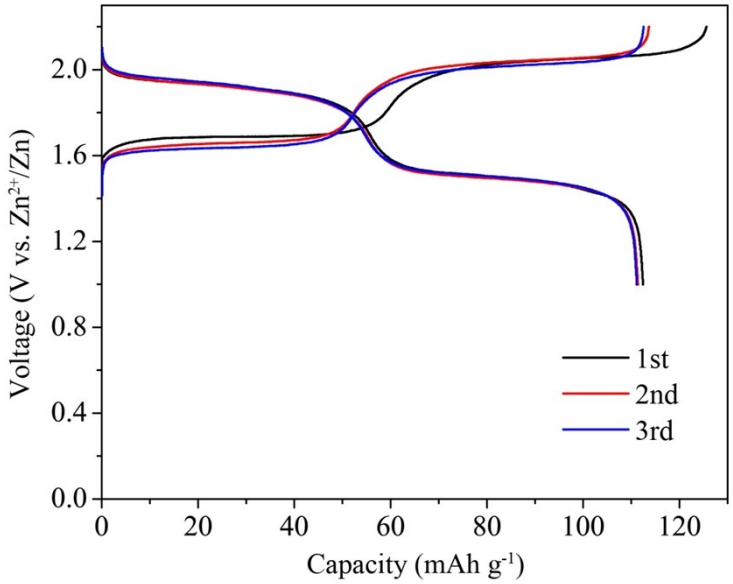

Fig. S21 Typical voltage profile of the Zn-NVPOF cell at 0.2 C. The Zn:NVPOF mass ratio is 0.21:1 (with 130% Zn) according to the theoretical capacity of Zn anode (820 mAh g^{-1}) and NVPOF cathode (130 mAh g^{-1}).

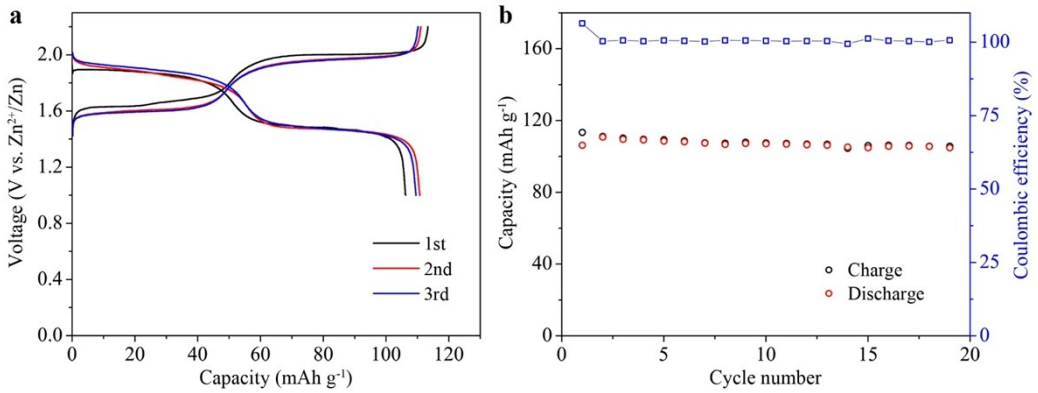

Fig. S22 (**a**) Typical discharge/charge curves and (**b**) cycling performance of the Zn-$NaV_2(PO_4)_2O_2F$ cell at 0.2 C.

We have attempted to estimate the full-cell energy density based on the total mass of the cathode**,** anode, and electrolyte, and an energy density of 59.5 Wh kg^{-1} is achieved. The calculation details are described below:

The density of the 0.2 M Zn^{2+} + 3.0 M Na^+ electrolyte is 1.31 g mL^{-1}.

1 mol e^- = 96500 C, 1 C = 1/3.6 mAh.

The full discharge of n g cathode material theoretically contributes to a capacity of 130n mAh, corresponding to $4.85n\times10^{-3}$ mol e^- ($(130n\times3.6)/96500 = 4.85n\times10^{-3}$), which needs $4.85n\times10^{-3}$ mol Na^+ in electrolyte. Thus, the volume of electrolyte (0.2 M Zn^{2+} + 3.0 M Na^+) theoretically needs 1.62n mL ($4.85n\times10^{-3}/3 = 1.62n\times10^{-3}$ L = 1.62n mL), and the mass of 1.62n mL electrolyte is 2.12n g ($1.62n\times1.31=2.12n$).

The average output voltage is 1.8 V with a reversible capacity of 110 mAh g^{-1}, corresponding to an energy density of 198 Wh kg^{-1} based on the cathode mass.

Therefore, the energy density can be calculated to be 59.5 Wh kg^{-1} based on the total weight of the cathode, anode and electrolyte ($198n/(n+0.21n+2.12n)$ = 59.5 Wh kg^{-1}).

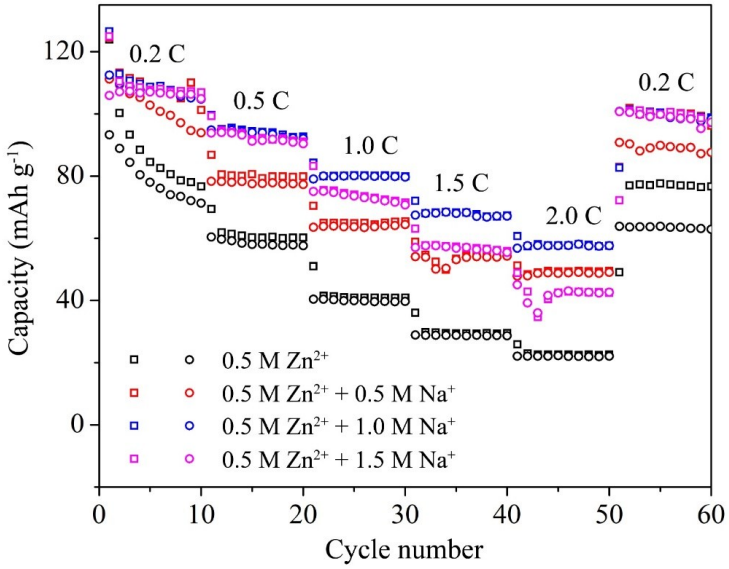

Fig. S23 Rate performances comparison of Zn/NVPOF cells in 0.5 M Zn^{2+}, 0.5 M Zn^{2+} + 0.5 M Na^{+}, 0.5 M Zn^{2+} + 1.0 M Na^{+}, and 0.5 M Zn^{2+} + 1.5 M Na^{+} electrolytes at various rates from 0.2 C to 2.0 C.

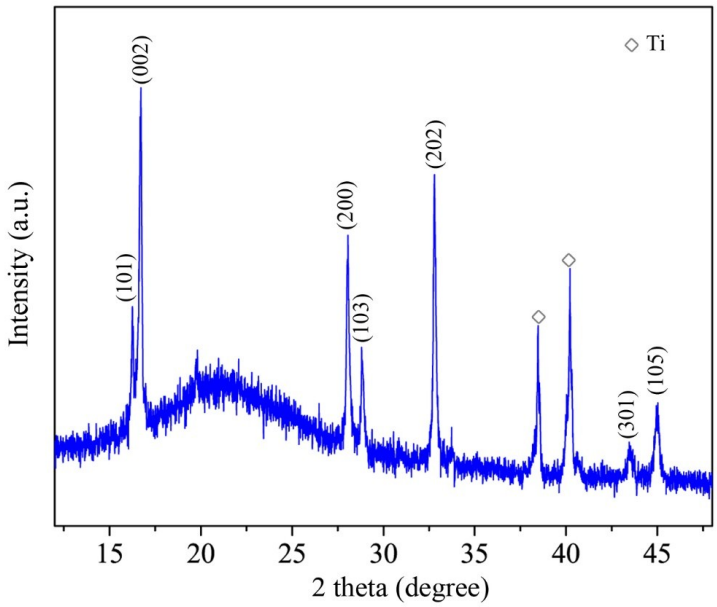

Fig. S24 XRD pattern of the NVPOF cathode after the rate test.

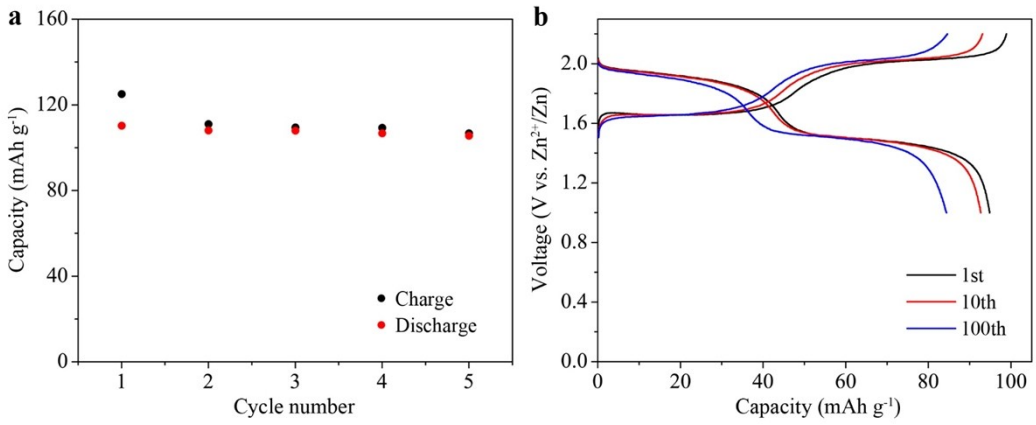

Fig. S25 (**a**) The initial five cycles of the Zn/NVPOF cell at 0.2 C. (**b**) Typical voltage profiles of the Zn/NVPOF cell at 1.0 C in the 0.5 M Zn^{2+} + 1.0 M Na^{+} electrolyte.

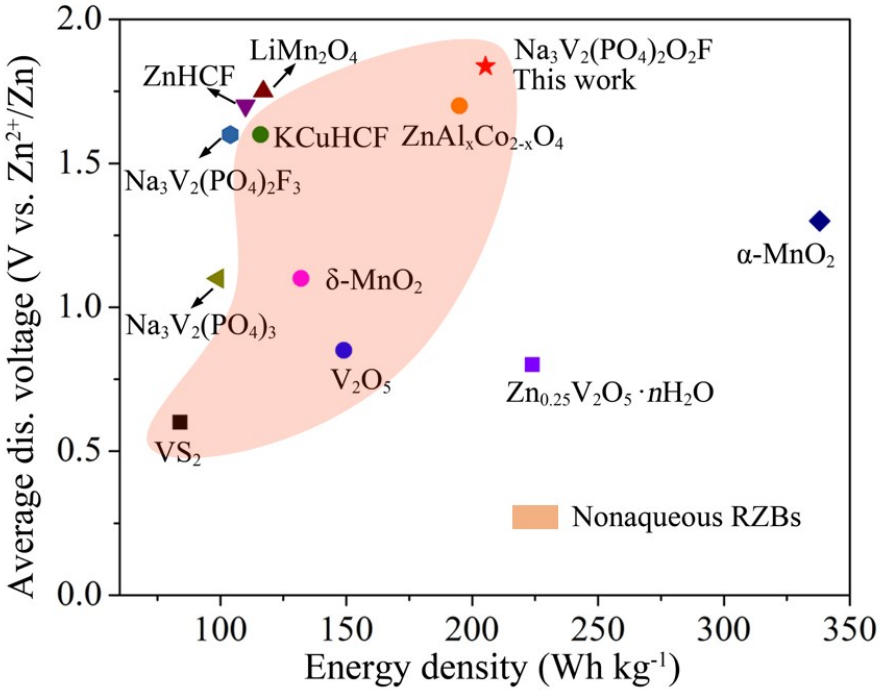

Fig. S26 Electrochemical comparison. Comparison of the average discharge (dis.) voltage and energy density of this Zn/NVPOF battery with the reported RZBs based on other cathode materials (e.g., α-MnO_2[1], δ-MnO_2[2], V_2O_5[3], VS_2[4], $Zn_{0.25}V_2O_5{\cdot}nH_2O$[5], ZnHCF[6], $Na_3V_2(PO_4)_3$[7], $Na_3V_2(PO_4)_2F_3$[8], $LiMn_2O_4$[9], KCuHCF[10], $ZnAl_xCo_{2-x}O_4$[11]). The light red region corresponds to the nonaqueous RZBs.

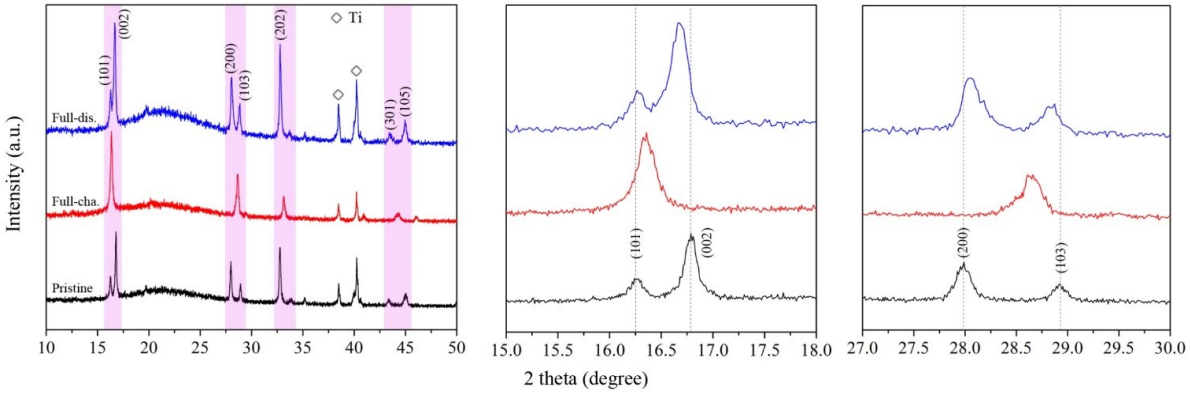

Fig. S27 XRD patterns of the NVPOF cathode in the 0.5 M Zn^{2+} electrolyte at the pristine, fully charged and discharged states.

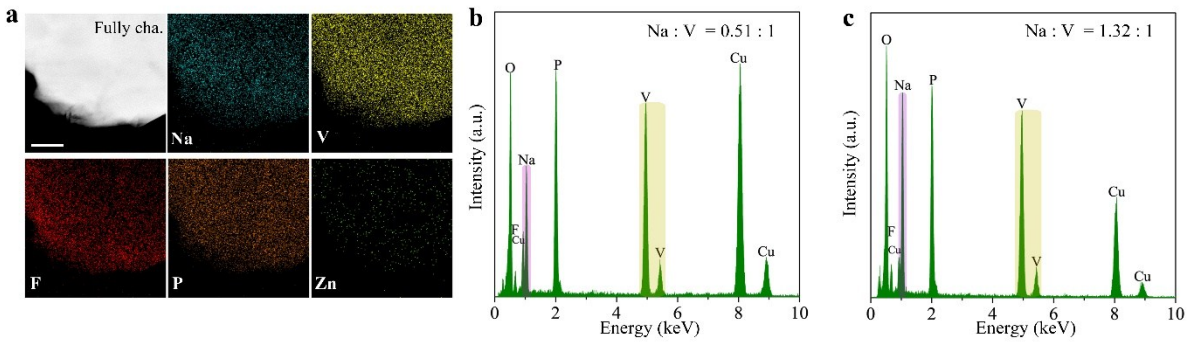

Fig. S28 (**a**) STEM images with the corresponding elements (e.g., Na, V, F, P, Zn) mapping images at the first fully charged state. TEM-EDS analyses of NVPOF cathodes at the first fully (**b**) charged and (**c**) discharged states. Scale bars, 500 nm.

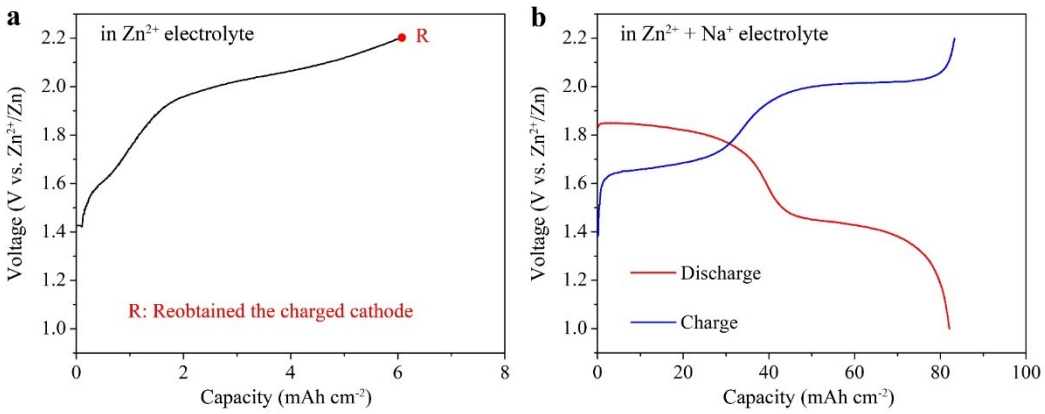

Fig. S29 (**a**) The typical charge profile of the first recovered $Na_{3-x}V_2(PO_4)_2O_2F$-1st cathode in the neat Zn^{2+} electrolyte at 0.2 C. The fully charged cathode ($Na_{3-x}V_2(PO_4)_2O_2F$-2nd) was reobtained and then thoroughly washed with TMP solvents. (**b**) Discharge/charge curves of the reobtained $Na_{3-x}V_2(PO_4)_2O_2F$-2nd cathode in the fresh 0.5 M Zn^{2+} + 1.0 M Na^+ electrolyte.

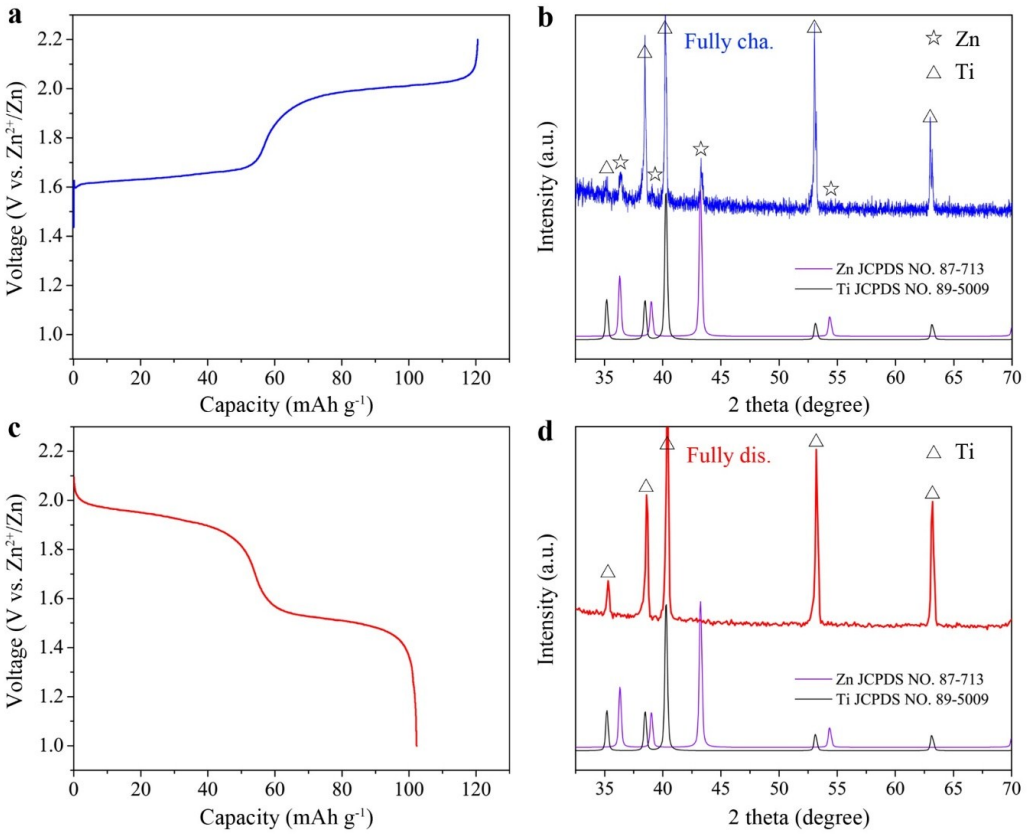

Fig. S30 Reaction mechanism of the anode side. The first (**a**) charge and (**c**) discharge curves of the Ti/NVPOF cells in the 0.5 M Zn^{2+} + 1 M Na^{+} electrolyte using Ti foil as the anode and NVPOF as the cathode at 0.2 C. After fully charged or discharged, the Ti foil was reobtained and then thoroughly washed with TMP solvents. XRD pattern of the recovered Ti foils at the fully (**b**) charged and (**d**) discharged states.

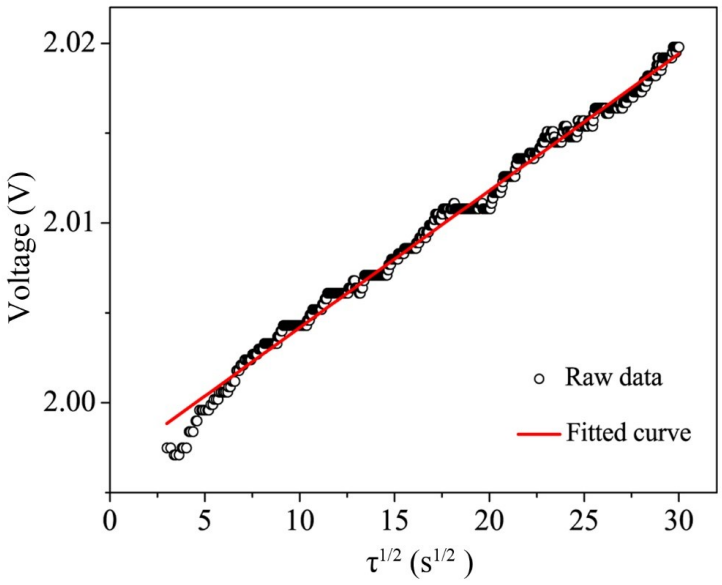

Fig. S31 Linear relationship between ΔE_τ and $\tau^{1/2}$.

For GITT test, the cell was charged or discharged at 30 mA g^{-1} with a duration time of 15 min and then relaxed for 60 min to allow the voltage equilibrium. This procedure was repeated for the full working window. A linear behavior is observed between the variation of the cell voltage (ΔE_τ) and the square root of the applied galvanostatic time ($\tau^{1/2}$), as shown in Fig. S31. The Na^+ diffusion coefficient (D_{Na}) can be calculated based on the equation: $D_{Na} = \frac{4}{\pi\tau}\left(\frac{m_B V_M}{M_B A}\right)^2\left(\frac{\Delta E_S}{\Delta E_\tau}\right)^2$, where m_B, M_B, V_M, A, and ΔE_s are the active material mass, molecular weight (g/mol), molar volume (cm^3/mol), active surface of the electrode, and the change of steady-state voltage for the corresponding step, respectively.[12,13]

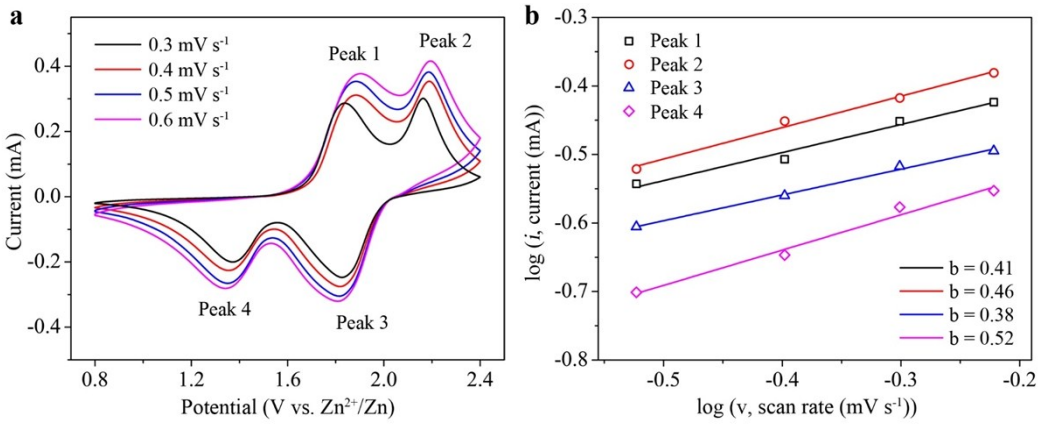

Fig. S32 (**a**) CV profiles of the NVPOF cathode at various sweep rates and (**b**) the corresponding log *i* vs log *v* plots at different oxidation/reduction states. When *b* value is close to 1.0, the redox reaction is mainly controlled by the capacitance, and when *b* value approaches 0.5, the reaction process is dominated by the Faradaic ion intercalation.

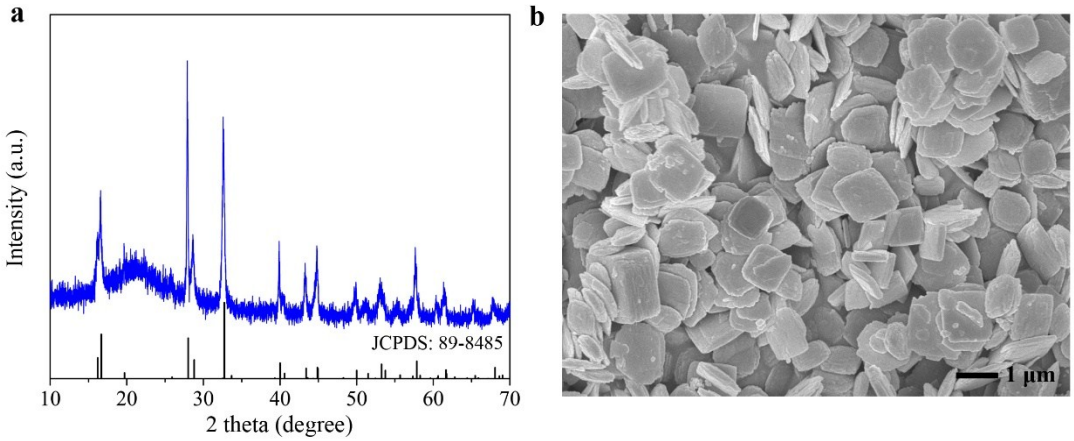

Fig. S33 Characterizations of the as-prepared $Na_3V_2(PO_4)_2F_3$. (**a**) XRD pattern and (**b**) SEM image.

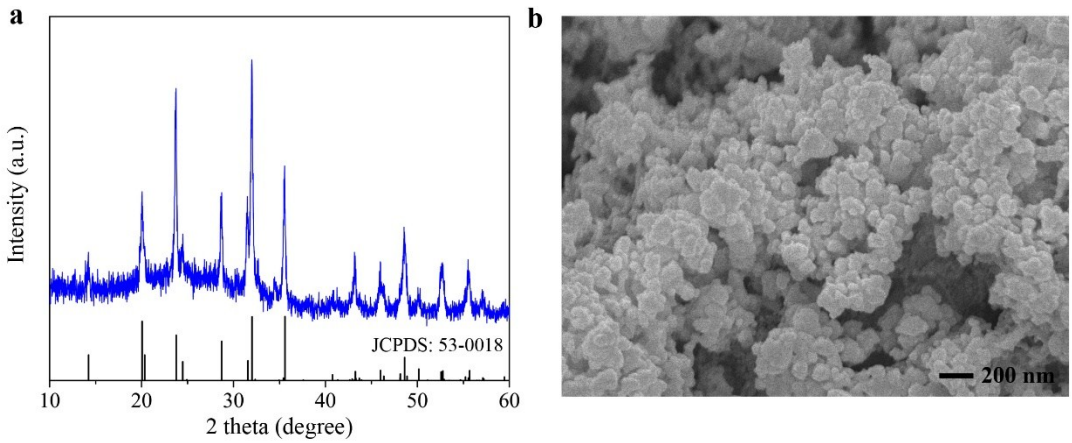

Fig. S34 Characterizations of the as-prepared $Na_3V_2(PO_4)_3$. (**a**) XRD pattern and (**b**) SEM image.

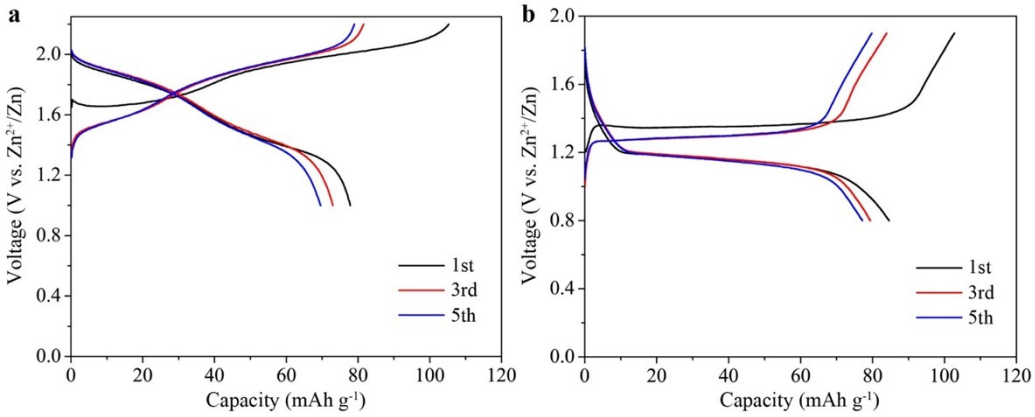

Fig. S35 Typical charge/discharge profiles of the (**a**) $Na_3V_2(PO_4)_2F_3$ cathode at 0.5 C and (**b**) $Na_3V_2(PO_4)_3$ cathode at 0.2 C in the neat 0.5 M Zn^{2+} electrolyte.

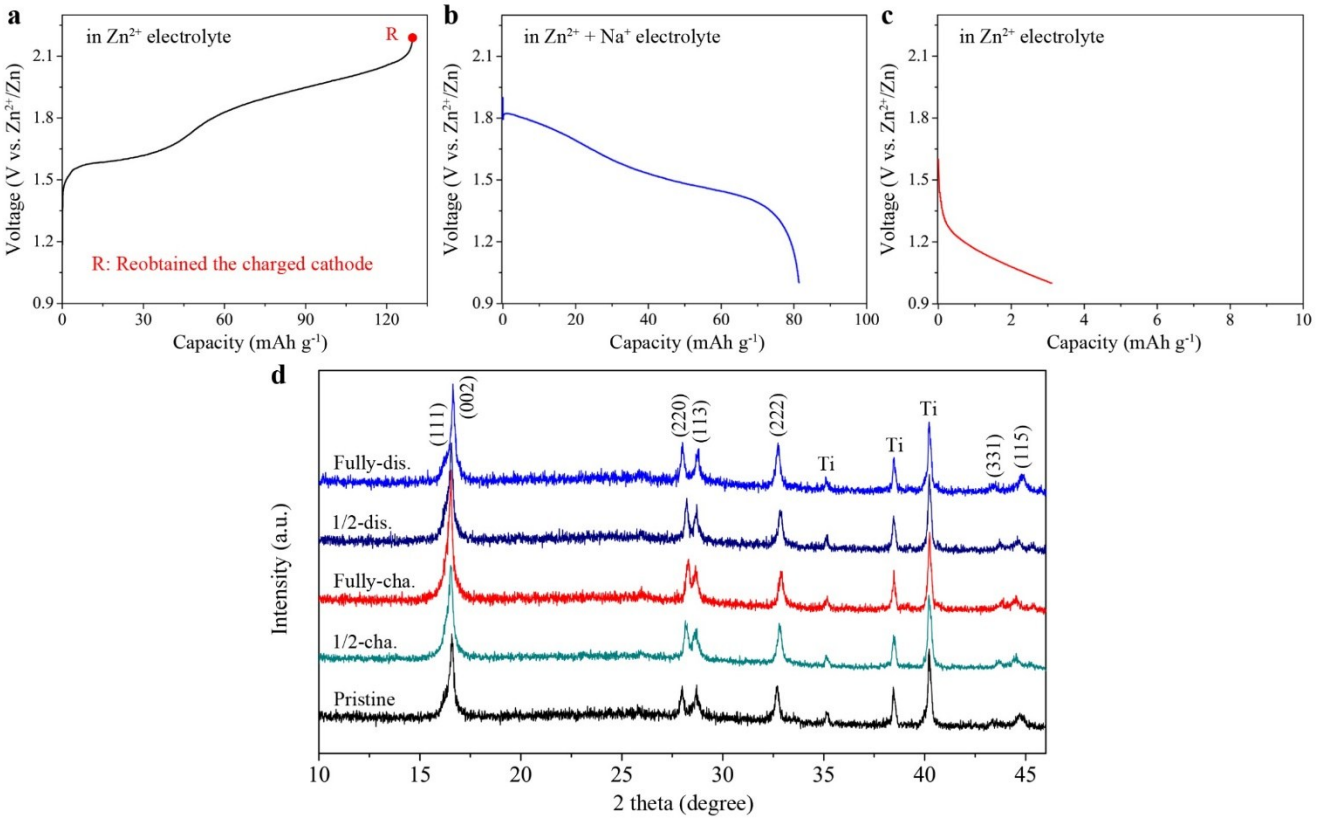

Fig. S36 Reaction mechanism. The first charge profile of $Na_3V_2(PO_4)_2F_3$ cathode in (**a**) the neat 0.5 M Zn^{2+} electrolyte and typical discharge curves of the recovered $Na_{3-x}V_2(PO_4)_2F_3$ cathodes in (**b**) fresh 0.5 M Zn^{2+} + 1.0 M Na^+ and (**c**) 0.5 M Zn^{2+} electrolytes at 0.2 C. (**d**) XRD patterns at selected states.

Firstly, the $Na_3V_2(PO_4)_2F_3$ cathode was charged to 2.2 V in the 0.5 M Zn^{2+} electrolyte, and then the charged $Na_3V_2(PO_4)_2F_3$ electrode was recovered and washed thoroughly with TMP solvents (Fig. S36a). The reobtained $Na_{3-x}V_2(PO_4)_2F_3$ cathode was re-assembled with a fresh Zn anode and a fresh 0.5 M Zn^{2+} + 1.0 M Na^+ or a neat 0.5 M Zn^{2+} electrolyte for subsequent discharge tests. In the dual-cations electrolyte, the $Na_{3-x}V_2(PO_4)_2F_3$ cathode exhibits a discharged capacity of ~82 mAh g^{-1} (Fig. S36b). However, in the neat 0.5 M Zn^{2+} electrolyte, the re-assembled cell shows no discharge platform with a negligible capacity of 3.2 mAh g^{-1} (Fig. S36c). In addition, ex-situ XRD analysis shows that the crystal structure evolution of $Na_3V_2(PO_4)_2F_3$ cathode is highly reversible during charge/discharge processes, similar to the case in sodium-ion battery system.[14,15] These results demonstrate that Na^+ cations reversibly intercalate into the $Na_3V_2(PO_4)_2F_3$ cathode without Zn^{2+} co-intercalation in this dual-cations electrolyte.

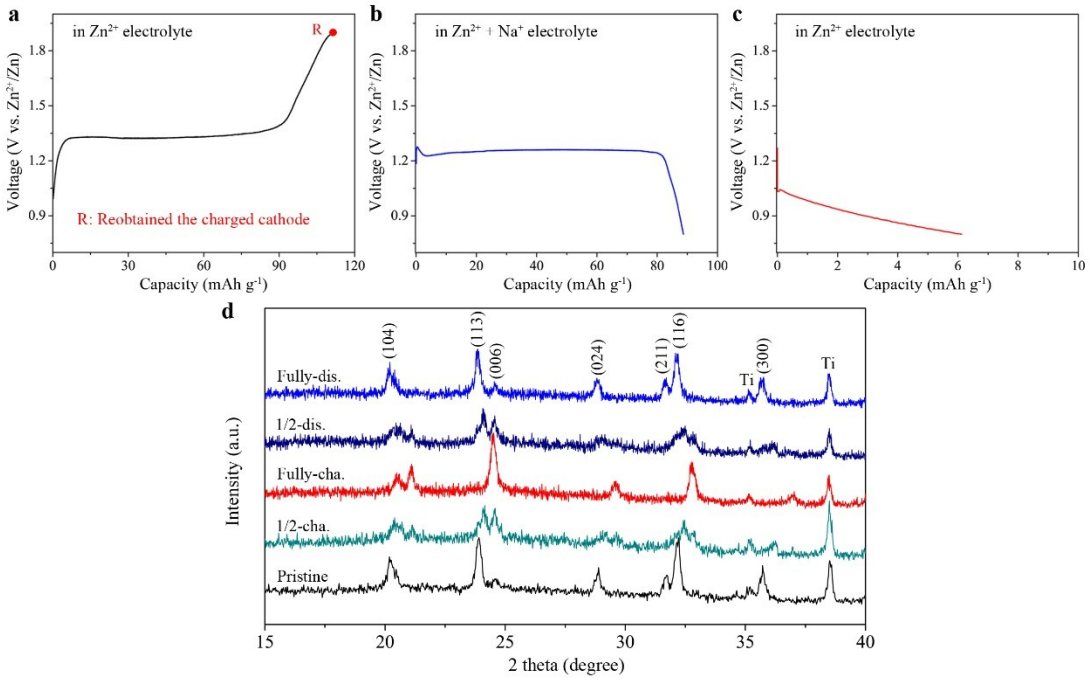

Fig. S37 Reaction mechanism. The first charge profile of $Na_3V_2(PO_4)_3$ cathode in (**a**) the neat 0.5 M Zn^{2+} electrolyte and typical discharge curves of the recovered $Na_{3-x}V_2(PO_4)_3$ cathodes in (**b**) fresh 0.5 M Zn^{2+} + 1.0 M Na^+ and (**c**) 0.5 M Zn^{2+} electrolytes at 0.2 C. (**d**) XRD patterns at selected states.

The $Na_3V_2(PO_4)_3$ cathode was firstly charged to 1.9 V in the 0.5 M Zn^{2+} electrolyte, and then the charged $Na_3V_2(PO_4)_3$ electrode was re-obtained and washed thoroughly with TMP solvents (Fig. S37a). The recovered $Na_{3-x}V_2(PO_4)_3$ electrode was re-assembled with a fresh Zn anode and a fresh 0.5 M Zn^{2+} + 1 M Na^+ or a neat 0.5 M Zn^{2+} electrolyte for subsequent discharge tests. In 0.5 M Zn^{2+} + 1.0 M Na^+ electrolyte, the $Na_{3-x}V_2(PO_4)_3$ cathode exhibits a discharged capacity of ~89 mAh g^{-1} with an evident platform (Fig. S37b). However, in the neat 0.5 M Zn^{2+} electrolyte, the re-assembled cell shows no discharge platform with a negligible capacity of 6.2 mAh g^{-1} (Fig. S37c). In addition, ex-situ XRD test shows that the structural evolution of $Na_3V_2(PO_4)_3$ cathode is highly reversible during charge/discharge processes, similar to that in the case in sodium-ion battery.[16] These results demonstrate that Na^+ cations reversibly intercalate into the $Na_3V_2(PO_4)_3$ cathode without Zn^{2+} co-intercalation in this dual-cations electrolyte.

Supplementary References

(1) H. Pan, Y. Shao, P. Yan, Y. Cheng, K. S. Han, Z. Nie, C. Wang, J. Yang, X. Li, P. Bhattacharya, K. T. Mueller and J. Liu, *Nat. Energy*, 2016, **1**, 16039.

(2) S.-D. Han, S. Kim, D. Li, V. Petkov, H. D. Yoo, P. J. Phillips, H. Wang, J. J. Kim, K. L. More, B. Key, R. F. Klie, J. Cabana, V. R. Stamenkovic, T. T. Fister, N. M. Markovic, A. K. Burrell, S. Tepavcevic and J. T. Vaughey, *Chem. Mater.*, 2017, **29**, 4874–4884.

(3) P. Senguttuvan, S.-D. Han, S. Kim, A. L. Lipson, S. Tepavcevic, T. T. Fister, I. D. Bloom, A. K. Burrell and C. S. Johnson, *Adv. Energy Mater.*, 2016, **6**, 1600826.

(4) A. Naveed, H. Yang, Y. Shao, J. Yang, N. Yanna, J. Liu, S. Shi, L. Zhang, A. Ye, B. He and J. Wang, *Adv. Mater.*, 2019, **31**, 1900668.

(5) D. Kundu, B. D. Adams, V. Duffort, S. H. Vajargah and L. F. Nazar, *Nat. Energy*, 2016, **1**, 16119.

(6) L. Zhang, L. Chen, X. Zhou and Z. Liu, *Adv. Energy Mater.*, 2015, **5**, 1400930.

(7) G. Li, Z. Yang, Y. Jiang, C. Jin, W. Huang, X. Ding and Y. Huang, *Nano Energy*, 2016, **25**, 211–217.

(8) W. Li, K. Wang, S. Cheng and K. Jiang, *Energy Storage Mater.*, 2018, **15**, 14–21.

(9) F. Wang, O. Borodin, T. Gao, X. Fan, W. Sun, F. Han, A. Faraone, J. A. Dura, K. Xu and C. Wang, *Nat. Mater.*, 2018, **17**, 543–549.

(10) A. Naveed, H. Yang, J. Yang, Y. Nuli and J. Wang, *Angew. Chem., Int. Ed.*, 2019, **28**, 2760–2764.

(11) C. Pan, R. G. Nuzzo and A. A. Gewirth, *Chem. Mater.*, 2017, **29**, 9351–9359.

(12) N. Zhang, M. Jia, Y. Dong, Y. Wang, J. Xu, Y. Liu, L. Jiao and F. Cheng, *Adv. Funct. Mater.*, 2019, **29**, 1807331.

(13) C. Xia, J. Guo, Y. Lei, H. Liang, C. Zhao and H. N. Alshareef, *Adv. Mater.*, 2018, **30**, 1705580.

(14) J.-Z. Guo, P.-F. Wang, X.-L. Wu, X.-H. Zhang, Q. Yan, H. Chen, J.-P. Zhang and Y.-G. Guo, *Adv. Mater.*, 2017, **29**, 1701968.

(15) Z. Jian, Y.-S. Hu, X. Ji and W. Chen, *Adv. Mater.*, 2017, **29**, 1601925.

(16) W. Duan, Z. Zhu, H. Li, Z. Hu, K. Zhang, F. Cheng and J. Chen, *J. Mater. Chem. A*, 2014, **2**, 8668–8675.